

LETTER TO THE EDITOR

Binary star progenitors of long gamma-ray bursts

M. Cantiello¹, S.-C. Yoon², N. Langer¹ and M. Livio³

¹ Institute for Astronomy (IfA) Astronomical Institute, Utrecht University, Princetonplein 5, 3584 CC, Utrecht, The Netherlands
e-mail: m.cantiello@astro.uu.nl

² Astronomical Institute Anton Pannekoek, University of Amsterdam, Kruislaan 403, 1098 SJ, Amsterdam, The Netherlands
e-mail: scyoon@science.uva.nl

³ Space Telescope Science Institute, 3700 San Martin Drive, Baltimore, MD 21218

Received 17 January 2007 / Accepted 20 February 2007

ABSTRACT

Context. The collapsar model for long gamma-ray bursts requires a rapidly rotating Wolf-Rayet star as progenitor.

Aims. We test the idea of producing rapidly rotating Wolf-Rayet stars in massive close binaries through mass accretion and consecutive quasi-chemically homogeneous evolution — the latter had previously been shown to provide collapsars below a certain metallicity threshold.

Methods. We use a 1-D hydrodynamic binary evolution code to simulate the evolution of a 16+15 M_⊙ binary model with an initial orbital period of 5 days and SMC metallicity (Z=0.004). Internal differential rotation, rotationally induced mixing and magnetic fields are included in both components, as well as non-conservative mass and angular momentum transfer, and tidal spin-orbit coupling.

Results. The considered binary system undergoes early Case B mass transfer. The mass donor becomes a helium star and dies as a Type Ib/c supernova. The mass gainer is spun-up, and internal magnetic fields efficiently transport accreted angular momentum into the stellar core. The orbital widening prevents subsequent tidal synchronization, and the mass gainer rejuvenates and evolves quasi-chemically homogeneously thereafter. The mass donor explodes 7 Myr before the collapse of the mass gainer. Assuming the binary to be broken-up by the supernova kick, the potential gamma-ray burst progenitor would become a runaway star with a space velocity of 27 km s⁻¹, traveling about 200 pc during its remaining lifetime.

Conclusions. The binary channel presented here does not, as such, provide a new physical model for collapsar production, as the resulting stellar models are almost identical to quasi-chemically homogeneously evolving rapidly rotating single stars. However, it may provide a means for massive stars to obtain the required high rotation rates. Moreover, it suggests that a possibly large fraction of long gamma-ray bursts occurs in runaway stars.

Key words. Stars: binary – Stars: rotation – Stars: evolution – Stars: mass-loss – Supernovae: general – Gamma rays: bursts

1. Introduction

Long gamma-ray bursts are thought to be produced by a subset of dying massive and possibly metal-poor stars (Jakobsson et al. 2005; Langer & Norman 2006; Modjaz et al. 2007). Within the currently favored collapsar scenario (Woosley 1993), the burst is produced by a rapidly rotating massive Wolf-Rayet (WR) star whose core collapses into a black hole (MacFadyen & Woosley 1999). While single star evolution models without internal magnetic fields can produce such configurations (Petrovic et al. 2005b; Hirschi et al. 2005), only models including magnetic fields are capable of reproducing the slow spins of young Galactic neutron stars (Heger et al. 2005; Ott et al. 2006) and white dwarfs (Suijs et al. 2007), due to the magnetic core-envelope coupling during the giant stage.

Various rather exotic binary evolution channels have been proposed to lead to long gamma-ray bursts (Fryer et al. 1999; Fryer & Heger 2005), supported by the idea that long gamma-ray bursts are very rare events (cf. Podsiadlowski et al. 2004). The recent realization that long gamma-ray bursts may have a bias towards low metallicity (e.g., Fynbo et al. 2003; Fruchter et al. 2006) may change the situation: rather than being exotic, GRBs may simply represent massive low-metallicity

stars — which locally are much rarer than O stars of solar metallicity (Langer & Norman 2006).

Yoon & Langer (2005), Yoon et al. (2006) and Woosley & Heger (2006) recently showed that below a certain metallicity threshold, very rapidly rotating single stars avoid the magnetic braking of the core through the so-called quasi-chemically homogeneous evolution: rotationally induced mixing processes keep the star close to chemical homogeneity, and thus the giant stage is avoided altogether. While these models are successful in producing models which fulfill all constraints of the collapsar model, they require very rapid initial rotation. The resulting number of long GRBs thus depends critically on the initial distribution of rotational velocities (IRF) of massive stars (Yoon et al. 2006).

The question thus arises whether the quasi-chemically homogeneous of massive stars can also be obtained in mass transferring massive binary systems (Vanbeveren & de Loore 1994), since in such systems the mass gainer can be spun-up to close to critical rotation (see Petrovic et al. 2005a,b), independent of its initial rotation rate. While Petrovic et al. (2005b) addressed this question and obtained a negative result, they used restrictive semiconvective mixing. As discussed in Yoon et al. (2006), the semiconvective mixing efficiency is still weakly constrained, but most recent stellar evolution models apply efficient semiconvec-

tive mixing. Thus, here we readdress the question, using models with efficient semiconvective mixing, as in Yoon et al. (2006).

2. Method

Our stellar model is calculated with the same hydrodynamic stellar evolution code as in Yoon et al. (2006). This includes the effect of rotation on the stellar structure, transport of angular momentum and chemical species via magnetic torques and rotationally induced hydrodynamic instabilities. Stellar wind mass loss, in particular metallicity dependent Wolf-Rayet mass loss, and enhancement of mass loss due to rapid rotation, have been included as in Yoon et al. (2006).

The binary evolution physics of our code is described in Petrovic et al. (2005a,b). It includes tidal coupling, mass and angular momentum transfer, and thermohaline mixing. The mass transfer efficiency is determined by the angular momentum balance of the accreting star: The amount of accreted matter is limited by the constraint that the angular momentum which it carries does not drive the rotation of the star beyond critical rotation (Petrovic et al. 2005a). To determine the accreted angular momentum, the code solves the equation of motion of test particles leaving the mass donor into a Roche potential (cf. also Dessart et al. 2003).

Here, we apply efficient semiconvective mixing; i.e., a value of $\alpha_{SM} = 1.0$ (cf. Langer et al. 1985) is used in the calculations discussed below. However, the same binary model as discussed below was also computed with $\alpha_{SM} = 0.1$ and $\alpha_{SM} = 0.01$.

3. Results

We compute the evolution of a binary system with rotating and magnetic components of $16 M_{\odot}$ and $15 M_{\odot}$, and an initial orbital period of 5 days. We chose an early Case B system with an initial mass ratio close to one for two reasons. Firstly, the expected mass transfer efficiency for this case was about 60% (meaning that 60% of the transferred matter can be retained by the mass gainer), based on the calculations by Wellstein (2001), Langer et al. (2004), and Petrovic et al. (2005a). Secondly, a Case B rather than Case A system was chosen to avoid synchronization *after* the major mass transfer phase.

The evolution of the binary system proceeded as follows (cf. Table 1). The initial rotational velocity of both stars has been set to 230 km s^{-1} , but both stars synchronize with the orbital rotation within about 1 Myr, to equatorial rotational velocities of only about 50 km s^{-1} (cf. Fig. 2). Rotationally induced mixing before the onset of mass transfer is thus negligible — in contrast to typical O stars evolving in isolation (Heger & Langer 2000; Meynet & Maeder 2000). The initially more massive star ends core hydrogen burning after $\sim 9.89 \text{ Myr}$, and Case B mass transfer begins shortly thereafter. It sheds about $12 M_{\odot}$ evolving into a $\sim 4 M_{\odot}$ helium star. About 1.5 Myr later, it sheds another $\sim 0.2 M_{\odot}$ as a helium giant, before exploding as Type Ib/c supernova.

The mass gainer keeps about $6 M_{\odot}$ of the overflowing matter, rendering the mass accretion efficiency to roughly 50%. Thereafter, it enters a phase of close-to-critical rotation, which induces rejuvenation and quasi-chemically homogeneous evolution (Figs. 2 and 3). Its mass loss is enhanced by rotation. About 5 Myr after the onset of accretion, the surface helium mass fraction of the mass gainer is increased to values above 60%, and Wolf-Rayet mass loss is assumed from then on. The star finishes core hydrogen burning after another 3 Myr, at an age of

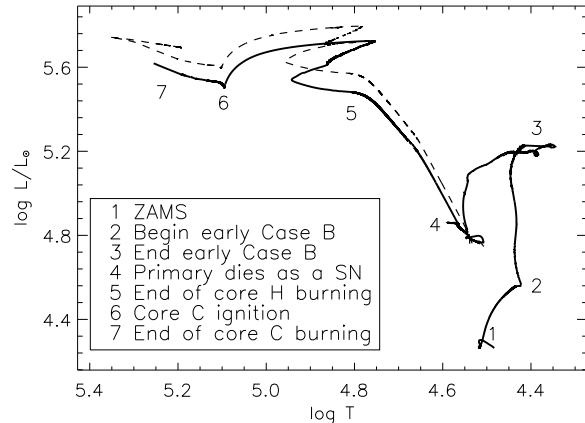


Fig. 1. Evolutionary track of the mass gainer in our $16 M_{\odot} + 15 M_{\odot}$ early Case B binary model (5 d initial orbital period) in the HR diagram (solid line), from the zero age main sequence up to core carbon exhaustion. The main evolutionary phases are labeled by numbers (see legend). The dashed line shows the evolutionary track of a very rapidly rotating ($v_{\text{init}}/v_K = 0.9$) $24 M_{\odot}$ single star. Both stars have SMC metallicity, and undergo quasi-chemically homogeneous evolution (see text).

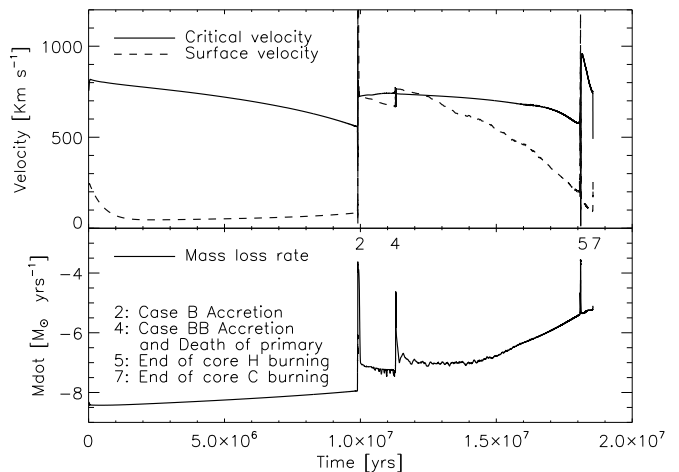


Fig. 2. **Upper panel:** Equatorial rotation velocity (dashed line) and critical rotation velocity (solid line) of the mass gainer of the computed $16 M_{\odot} + 15 M_{\odot}$ early Case B binary sequence, as function of time, from the zero-age main sequence until core carbon exhaustion. **Lower panel:** Mass loss rate of the same stellar model, as function of time. The numbered evolutionary stages correspond to those given in Fig. 1 and Tab. 1

18.1 Myr , with a mass of $16.8 M_{\odot}$, a surface helium mass fraction of 95%, and rotating with $\sim 200 \text{ km s}^{-1}$.

After core hydrogen exhaustion, the mass gainer contracts and spins-up to critical rotation, which leads to a mass shedding of almost $2 M_{\odot}$. During its remaining lifetime of less than 0.5 Myr, it loses about another $2 M_{\odot}$ to a Wolf-Rayet wind. It ends its life as a rapidly rotating Wolf-Rayet star with a final mass of about $13 M_{\odot}$, ready to form a collapsar. Assuming the binary broke up upon the explosion of the mass loser, the mass gainer would have traveled for about 7 Myr with its final orbital velocity of 27 km s^{-1} a distance of about 200 pc.

Table 1. Major evolutionary phases of the computed $16 M_{\odot} + 15 M_{\odot}$ early Case B binary sequence. The binary calculation ends after core carbon exhaustion of the mass loser (the primary), and the mass gainer (the secondary) is then evolved as a single star. We show evolutionary time, masses of both stars, mass lost from the system, orbital period, surface rotational velocities, central and surface helium mass fraction of the mass gainer, and orbital velocities of both stars. The abbreviations for the evolutionary phases are: ZAMS = zero age main sequence; ECHB = end core hydrogen burning; ICB = ignition of carbon burning; ECCB = end core carbon burning. The numbered evolutionary stages correspond to those given in Fig. 1 and Fig. 2

Phase	Time Myr	M_1 M_{\odot}	M_2 M_{\odot}	ΔM M_{\odot}	P d	$v_{rot,1}$ km s^{-1}	$v_{rot,2}$ km s^{-1}	$Y_{c,2}$	$Y_{s,2}$	$v_{orbit,1}$ km s^{-1}	$v_{orbit,2}$ km s^{-1}
1 ZAMS	0	16	15	–	5.0	230	230	0.248	0.248	188	201
2 begin Case B	9.89	15.92	14.94	0.14	5.1	96	85	0.879	0.248	186	198
3 end Case B	9.90	3.93	20.77	6.30	38.2	27	719	0.434	0.348	153	29
4 ECCB primary	11.30	3.71	20.86	6.44	42.7	40	767	0.457	0.441	149	27
5 ECHB secondary	18.10	–	16.76	–	–	–	202	0.996	0.956	–	–
6 ICB secondary	18.56	–	12.85	–	–	–	191	0.000	0.996	–	–
7 ECCB secondary	18.56	–	12.83	–	–	–	258	0.000	0.996	–	–

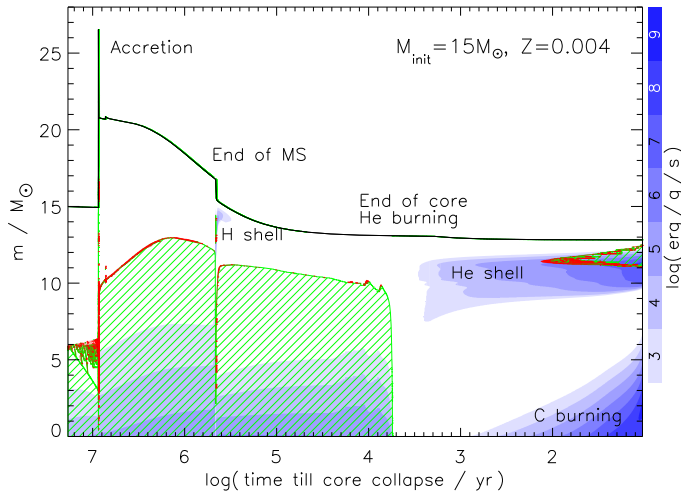


Fig. 3. Evolution of the internal structure of the mass gainer of the computed $16 M_{\odot} + 15 M_{\odot}$ early Case B binary sequence, as function of time, from the zero-age main sequence to core carbon exhaustion. The time axis is logarithmic, with the time of core collapse as zero point. Convective layers are hatched. Semiconvective layers are marked by dots (red dots in the electronic version). Gray (blue) shading indicates nuclear energy generation (color bar to the right of the figure). The topmost solid line denotes the surface of the star.

Following Brandt & Podsiadlowski (1995) we calculate the kick velocity necessary to unbind the binary system, under the hypothesis of instantaneous removal of the SN ejecta. Two extreme values correspond to the most and to the least efficient geometrical configuration for the supernova kick to break up the system. The minimum kick velocity is 52 km s^{-1} and corresponds to the case where the kick is aligned with the orbital velocity vector of the supernova progenitor. The maximum kick velocity necessary to unbind the system is 350 km s^{-1} , which is required if the kick is aligned to the orbital velocity vector, but directed backward. According to the observed velocity distribution of radio pulsars, about 55% of pulsars have a space velocity larger than 350 km s^{-1} , while more than 98% have a velocity above 52 km s^{-1} (Arzoumanian et al. 2002). In order to estimate the chance of obtaining a runaway star out of our system we performed a Monte Carlo simulation for a randomly oriented supernova kick. According to the observed velocity distribution of radio pulsars (Arzoumanian et al. 2002) the probability for the

Table 2. Average specific angular momentum in the CO core ($\langle j_{CO} \rangle$) for six different stellar evolution models, at the end of carbon core burning. The first three (labeled ‘binary’) correspond to the mass gainers of the computed $16 M_{\odot} + 15 M_{\odot}$ early Case B binary sequence, for three different values of the semiconvection parameter. The fourth corresponds to the computed $24 M_{\odot}$ single star with initially 90% of Keplerian velocity ($v_{init}/v_K = 0.9$). The last two correspond to the $20 M_{\odot}$ single star models with $Z=0.004$ and initially 60% and 30% of Keplerian rotation of Yoon et al. (2006). Models in bold face are evolving quasi-chemically homogeneous. The specific angular momentum of the least stable orbit around a $3 M_{\odot}$ Kerr black hole for these models is about $30 \times 10^{15} \text{ cm}^2 \text{ s}^{-1}$.

Model	M_i M_{\odot}	α_{SM}	v_{init}/v_K	$\langle j_{CO} \rangle$ $10^{15} \text{ cm}^2 \text{ s}^{-1}$	M_{CO} M_{\odot}
binary	15	1.0	–	18.15	10.0
binary	15	0.1	–	8.90	8.4
binary	15	0.01	–	1.09	2.8
single	24	1.0	0.9	23.42	11.4
single	20	1.0	0.6	11.62	9.9
single	20	1.0	0.3	2.09	4.2

binary system to break up by the first supernova explosion is about 80%.

The same binary model as discussed above was also computed with $\alpha_{SM} = 0.1$ and $\alpha_{SM} = 0.01$. The first case mentioned practically reproduces the results outlined above, even if the CO core angular momentum content of the GRB progenitor is lower in this case (see Tab. 2). The second case confirmed the finding of Petrovic et al. (2005b) that chemically homogeneous evolution does not occur for restrictive semiconvective mixing.

4. Comparison to single star model

It is instructive to compare the evolution of the mass gainer of the binary model described above with that of a rapidly rotating single star of similar mass. Fig. 4 shows the Kippenhahn diagram of a $24 M_{\odot}$ single star with SMC metallicity with an initial rotation rate of 700 km s^{-1} , corresponding to 90% of Keplerian rotation ($v_{init}/v_K = 0.9$). Modeling details are as in Yoon et al. (2006). A comparison with Fig. 3 reveals that its evolution is almost identical to that of the mass gainer after accretion in the binary model described above. This similarity is underpinned by a comparison of the evolutionary tracks of both stars in the HR diagram

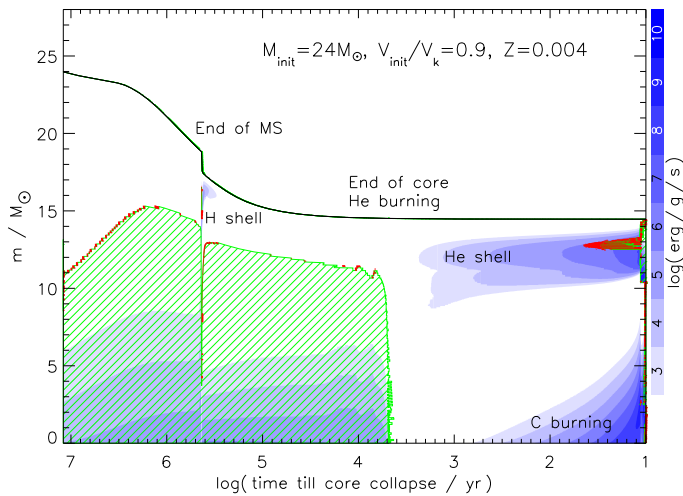


Fig. 4. Evolution of the internal structure of a single star model with initial mass of $24 M_{\odot}$ and initial rotation close to Keplerian ($v_{\text{init}}/v_{\text{K}}=0.9$). The evolution is shown from the zero-age main sequence to the end of O burning. Convective layers are hatched. Semi-convective layers are marked by dots (red dots in the electronic version). The gray (blue) shading gives nuclear energy generation rates in log scale, as indicated on the right side. The topmost solid line denotes the surface of the star.

(Fig. 1). Table 2 shows that also the final core angular momentum of the binary model is not significantly different from that of corresponding single stars.

As a consequence, one may conclude that the binary model does not, from the point of view of the internal stellar evolution, provide anything new or different from what is already obtained in rapidly rotating single stars. In particular, it can not be expected that the metallicity threshold for obtaining a long gamma-ray burst (cf. Yoon et al. 2006) can be significantly increased through the type of binary evolution considered here. While a rejuvenated accreting star is somewhat more evolved than a zero-age main sequence star, this difference is small and leads only to the avoidance of a small fraction of the mass loss induced spin-down during core hydrogen burning. However, it is to be said that single stars which rotate initially with 90% of their break-up velocity might not form in nature (cf. Mokiem et al. 2006, and see below). Thus, perhaps the main benefit of the massive close binaries is just to produce very rapidly rotating O stars.

5. Discussion

The binary evolution model presented above shows that quasi-chemically homogeneous evolution may occur in mass gainers of low-metallicity massive early Case B binaries. The comparison of the mass gainer with a corresponding single star model made it clear that such binary components evolve in the same way as extremely rapidly rotating single stars. This confirms that the scenario of quasi-chemically homogeneous evolution might not be restricted to single stars, but may apply to the accreting component of massive close binaries as well.

While we provide only one example, it seems likely that this scenario applies to most massive close binary components which accrete or gain an appreciable amount of mass; this may encompass Case A binaries and early Case B binaries (Podsiadlowski et al. 1992; Wellstein & Langer 1999; Wellstein et al. 2001). Case A merger are also likely contributing to this scenario. While the merged object will have more

mass than the initially more massive star in the binary, the product will be extremely rapidly rotating due to the orbital angular momentum, as in the case of some blue stragglers (Livio 1993).

5.1. Binaries and the distribution of rotational velocities

The best constraint so far on the distribution of initial rotational velocities (IRF) comes from the recent study of young O stars in the SMC, mostly from the cluster NGC 346 (Mokiem et al. 2006). According to Yoon et al. (2006), the three most rapid rotators from the sample of 21 O stars would qualify for the quasi-chemically homogeneous evolution scenario, and remarkably, all three stars are found to be helium-enhanced. The simplest approach to understand those stars is to assume that they correspond to the tip of the IRF.

However, that data of Mokiem et al. (2006) reveals another interesting feature: two of the the three mentioned stars are runaway stars, with radial velocities deviating by $30..70 \text{ km s}^{-1}$ from the average cluster radial velocity. While dealing with low number statistics, this information opens another possibility: that the most rapidly rotating young O stars in the SMC are products of binary evolution. A closer examination of the IRF derived by Mokiem et al. (2006) appears to support this idea: While the three rapid rotators show $v \sin i \gtrsim 290 \text{ km s}^{-1}$, all other stars have $v \sin i \lesssim 210 \text{ km s}^{-1}$.

The following hypothesis therefore seems conceivable: The IRF of single O stars in the SMC ends at about 210 km s^{-1} — too early to allow quasi-chemically homogeneous evolution and collapsar formation. However, massive close binary evolution enhances the IRF to what we may call the apparent IRF as measured by Mokiem et al. (2006), which leads to the redshift dependent GRB rate as worked out by Yoon et al. (2006). According to the binary population synthesis model of Podsiadlowski et al. (1992), about 10% of all massive binaries might lead to a Case A merger or early Case B mass transfer, which is sufficient to populate the rapidly rotating part of the IRF of Mokiem et al. In that context, the rapidly rotating O star in the sample of Mokiem et al. (2006) which does not appear as runaway star could either have an undetected high proper motion, or it could be the result of a Case A merger — where no runaway is produced.

5.2. Effects from runaway GRBs

The runaway nature of a GRB progenitor, as obtained in our example, has important observational consequences for both the positions of GRBs, and their afterglow properties. Concerning the afterglow, it is relevant that the medium close to a WR star has the density profile of a free-streaming wind, and analytical and numerical calculations both suggest that the free wind of a single WR typically extends over many parsec (van Marle et al. 2006). However, from the analysis of GRB afterglows, a constant circumstellar medium density has been inferred in many cases (Chevalier & Li 2000; Panaitescu & Kumar 2001, 2002; Chevalier et al. 2004). A possible explanation has been proposed by van Marle et al. (2006), who simulated the circumstellar medium around a moving WR star. As the GRB jet axis is likely perpendicular to the space velocity vector, the jet escapes through a region of the bow-shock where the wind termination shock is very close to the star. Therefore, the jet may enter a constant density medium quickly in this situation.

Concerning the GRB positions, since the spin axis of the stars in a close binary system are likely orthogonal to the or-

bit plane, the observation of a GRB produced by the proposed binary channel is possible only if the binary orbit is seen nearly face on. Then the direction of motion of the runaway GRB progenitor must be orthogonal to the line of sight, allowing the progenitor, for the given space velocity, to obtain the maximum possible apparent separation from its formation region. The finding of Hammer et al. (2006), that the nearest three long gamma-ray bursts may be due to runaway stars is in remarkable agreement with our scenario. While the collapsar progenitor in our binary model travels only 200 pc before it dies, compared to the 400...800 pc deduced by Hammer et al. (2006), binary evolution resulting in higher runaway velocities are certainly possible (Petrovic et al. 2005a). It remains to be analyzed whether the runaway scenario is compatible with the finding that long GRBs are more concentrated in the brightest regions of their host galaxies than core collapse supernovae (Fruchter et al. 2006).

Acknowledgements. We are grateful to the referee Stan Woosley, for his criticism which helped to significantly improve this paper. S.-C. Yoon is supported by the VENI grant (639.041.406) of the Netherlands Organization for Scientific Research (NWO).

References

- Arzoumanian, Z., Chernoff, D. F., & Cordes, J. M. 2002, *ApJ*, 568, 289
 Brandt, N. & Podsiadlowski, P. 1995, *MNRAS*, 274, 461
 Chevalier, R. A. & Li, Z.-Y. 2000, *ApJ*, 536, 195
 Chevalier, R. A., Li, Z.-Y., & Fransson, C. 2004, *ApJ*, 606, 369
 Dessart, L., Langer, N., & Petrovic, J. 2003, *A&A*, 404, 991
 Fruchter, A. S., Levan, A. J., Strolger, L., et al. 2006, *Nature*, 441, 463
 Fryer, C. L. & Heger, A. 2005, *ApJ*, 623, 302
 Fryer, C. L., Woosley, S. E., & Hartmann, D. H. 1999, *ApJ*, 526, 152
 Fynbo, J. P. U., Jakobsson, P., Möller, P., et al. 2003, *A&A*, 406, L63
 Hammer, F., Flores, H., Schaerer, D., et al. 2006, *A&A*, 454, 103
 Heger, A. & Langer, N. 2000, *ApJ*, 544, 1016
 Heger, A., Woosley, S. E., & Spruit, H. C. 2005, *ApJ*, 626, 350
 Hirschi, R., Meynet, G., & Maeder, A. 2005, *A&A*, 443, 581
 Jakobsson, P., Björnsson, G., Fynbo, J. P. U., et al. 2005, *MNRAS*, 362, 245
 Langer, N., El Eid, M. F., & Fricke, K. J. 1985, *A&A*, 145, 179
 Langer, N. & Norman, C. A. 2006, *ApJ*, 638, L63
 Langer, N., Yoon, S.-C., Petrovic, J., & Heger, A. 2004, in *IAU Symposium*, ed. A. Maeder & P. Eenens, P. 535
 Livio, M. 1993, in *ASP Conf. Ser. 53: Blue Stragglers*, ed. R. A. Saffer, 3–+
 MacFadyen, A. I. & Woosley, S. E. 1999, *ApJ*, 524, 262
 Meynet, G. & Maeder, A. 2000, *A&A*, 361, 101
 Modjaz, M., Kewley, R., Kirshner, R., et al. 2007, *astro-ph/0701246*, *AJ* submitted
 Mokiem, M. R., de Koter, A., Evans, C. J., et al. 2006, *A&A*, 456, 1131
 Ott, C. D., Burrows, A., Thompson, T. A., Livne, E., & Walder, R. 2006, *ApJS*, 164, 130
 Panaitescu, A. & Kumar, P. 2001, *ApJ*, 554, 667
 Panaitescu, A. & Kumar, P. 2002, *ApJ*, 571, 779
 Petrovic, J., Langer, N., & van der Hucht, K. A. 2005a, *A&A*, 435, 1013
 Petrovic, J., Langer, N., Yoon, S.-C., & Heger, A. 2005b, *A&A*, 435, 247
 Podsiadlowski, P., Joss, P. C., & Hsu, J. J. L. 1992, *ApJ*, 391, 246
 Podsiadlowski, P., Mazzali, P. A., Nomoto, K., Lazzati, D., & Cappellaro, E. 2004, *ApJ*, 607, L17
 Suijs, M., Langer, N., Yoon, S. C., Poelarends, A. J., & Heger, A. 2007, in prep
 van Marle, A. J., Langer, N., Achterberg, A., & Garcafa-Segura, G. 2006, *A&A*, 460, 105
 Vanbeveren, D. & de Loore, C. 1994, *A&A*, 290, 129
 Wellstein, S. 2001, PhD thesis, University of Potsdam
 Wellstein, S. & Langer, N. 1999, *A&A*, 350, 148
 Wellstein, S., Langer, N., & Braun, H. 2001, *A&A*, 369, 939
 Woosley, S. E. 1993, *ApJ*, 405, 273
 Woosley, S. E. & Heger, A. 2006, *ApJ*, 637, 914
 Yoon, S.-C. & Langer, N. 2005, *A&A*, 443, 643
 Yoon, S.-C., Langer, N., & Norman, C. 2006, *A&A*, 460, 199